Received: 17 December 2021 | Revised: 8 April 2022 | Accepted: 14 April 2022

DOI: 10.1002/hyp.14588

RESEARCH ARTICLE

WILEY

# Comparison of three different numerical implementations to model rainfall-runoff transformation on roofs

Esteban Sañudo | Luis Cea | Jerónimo Puertas

Universidade da Coruña, Water and Environmental Engineering Group, Department of Civil Engineering, School of Civil Engineering, A Coruña, Spain

**Correspondence**
Esteban Sañudo, Universidade da Coruña, Water and Environmental Engineering Group, Department of Civil Engineering, School of Civil Engineering, Elviña, 15071 A Coruña, Spain.
Email: e.sanudo@udc.es

**Funding information**
Ministerio de Ciencia e Innovación, Grant/Award Number: PID2020-118368RB-I00; Universidade da Coruña

## Abstract

Roofs represent a high percentage of the impervious surfaces in urban areas, and hence their implementation in urban drainage models is essential for accurate results to be achieved. Current modelling approaches are based on parameters such as a roof's slope and width, its roughness coefficient, and the initial abstraction. In this study, an experimental campaign was performed in order to assess the sensitivity of the roof runoff hydrographs to these parameters. The experimental tests were carried out in a new large-scale urban drainage facility equipped with a rainfall simulator. The experimental tests were replicated numerically using three different levels of model resolution, from a high fidelity representation with a spatial resolution of 5 mm (which can be considered a digital twin) to a lumped representation. Our experimental results show that, for practical purposes, the sensitivity of the outlet runoff hydrograph to the roof slope tested is negligible. The numerical upscaling analysis carried out showed that flat roofs present a slightly different hydrograph behaviour with greater times of concentration than sloped roofs. No significant sensitivity of the outlet hydrograph to the surface roughness coefficient was found. In terms of numerical modelling, the use of a very high spatial resolution for the roof, which implies a high computational cost, does not affect the results significantly compared to the far simpler lumped approach. The current research involves the first thorough experimental and computational analysis of the runoff over roofs to date.

**KEYWORDS**
Iber, LiDAR, numerical modelling, physical model, SWMM, urban drainage

## 1 | INTRODUCTION

The distribution of urban spaces typically sees a division into pervious areas, such as green spaces, and impervious ones, like roads and buildings. Green spaces replicate natural hydrology processes, whereas impervious areas modify completely the natural hydrological behaviour of a catchment, increasing surface runoff volumes and leading to negative impacts on the environment. Numerical urban drainage models are commonly used to understand the response of urban catchments during extreme rainfall events (Chang et al., 2015; Fraga et al., 2017; Leandro & Martins, 2016; Sañudo et al., 2020). These models implement a thorough representation of the different elements in an urban catchment, including sewers, streets, gullies, manholes and roofs. Whilst several studies have dealt with the representation of overland flow over urban surfaces, in sewers, and through the links between streets and sewers, the transformation of rainfall runoff over roofs has received far less attention. Nevertheless, building footprints constitute an important area within the total

impervious surface, and the contribution of the rainwater discharges from roofs to the drainage system is significant. Thus, it is essential to implement a correct representation of roofs in order to achieve accurate results (Cao et al., 2021). The modelling of roofs in urban drainage models is generally done using lumped approaches, in which their footprints are represented as void areas, and the rainfall-runoff transformation on the roof is computed using an algebraic equation (Pina et al., 2016). Kinematic wave equations were also used to model roof runoff (Silveira et al., 2016). The computed hydrograph is introduced directly as an inflow in the sewer network.

At the same time, the enhancement of urban drainage models and increases in computing power are making it possible to model urban geometries and topography with a very high spatial resolution, using fully distributed 2D models. Such an approach to modelling, however, demands a very accurate definition of the topography and high levels of computation. Both requirements can be achieved at the laboratory scale or in relatively small neighbourhoods, but at larger scales it is prohibitive to work at such detailed resolutions.

This study focuses on how the spatial representation of roofs in urban drainage models might affect the model results. To that end, a detailed high-resolution geometry of roofs was derived using LIDAR technology, and a rainfall-runoff experimental campaign was carried out in a large-scale urban drainage facility equipped with a rainfall simulator that can generate rain intensities of 30, 50, and 80 mm/h with high spatial uniformity. The output hydrographs at the end of the gutters were measured for different roof configurations and six hyetographs. The experiments were numerically modelled using three different levels of detail: (i) a digital twin resolution, where the surface runoff in the roofs is computed using the shallow water equations (2D-SWE) with very detailed 2D discretisation, one that includes a detailed definition of the geometry of the channel and ridge tiles, (ii) a simplified spatial resolution, in which the roof is modelled as a sloped plane also solving 2D-SWE, and (iii) a lumped approach based on the nonlinear reservoir equation. Finally, several full-size roofs were analysed numerically in order to assess the effect of upscaling on the concentration time.

## 2 | MATERIAL AND METHODS

### 2.1 | Description of the urban drainage facility

The urban drainage facility used in this study is located at the Hydraulics Laboratory of the Centre of Technological Innovation in Construction and Civil Engineering (CITEEC), University of A Coruña (Spain). The facility consists of a large-scale street intersection of 100 $m^2$ linked to a sewer network and equipped with a rainfall simulator. The street domain consists of two T-intersected concrete roadways, a tiled concrete pavement separated from the road by a 6 cm high curb, and four building blocks with tile roofs with different slopes (Figure 1). The roadway and pavements have 2% and 1% transversal and longitudinal slopes, respectively.

The rainfall simulator was built following the configuration developed and validated in Naves et al. (2020) and consists of 4500 pressure-compensating drippers of 1.2 and 2 L/h, these located over a grid that breaks and spreads the drops generated by the drippers. The drippers are inserted into two independent hydraulic circuits, each one forming a grid with longitudinal and transversal separation of 0.2 m. This configuration results in 25 drippers per $m^2$ per circuit. The rainfall simulator is able to generate highly homogeneous rainfall intensities of approximately 30, 50, and 80 mm/h over the 100 $m^2$

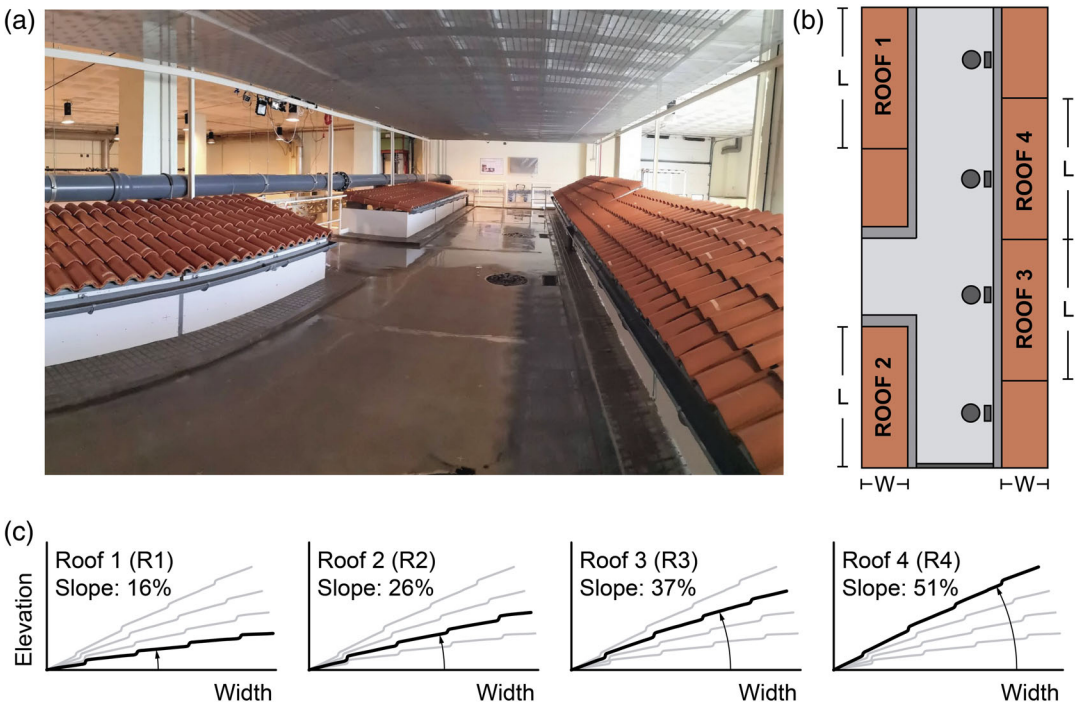


**FIGURE 1** (a) Experimental facility, (b) schematic representation of the roofs, and (c) transversal profiles and slopes of the roofs

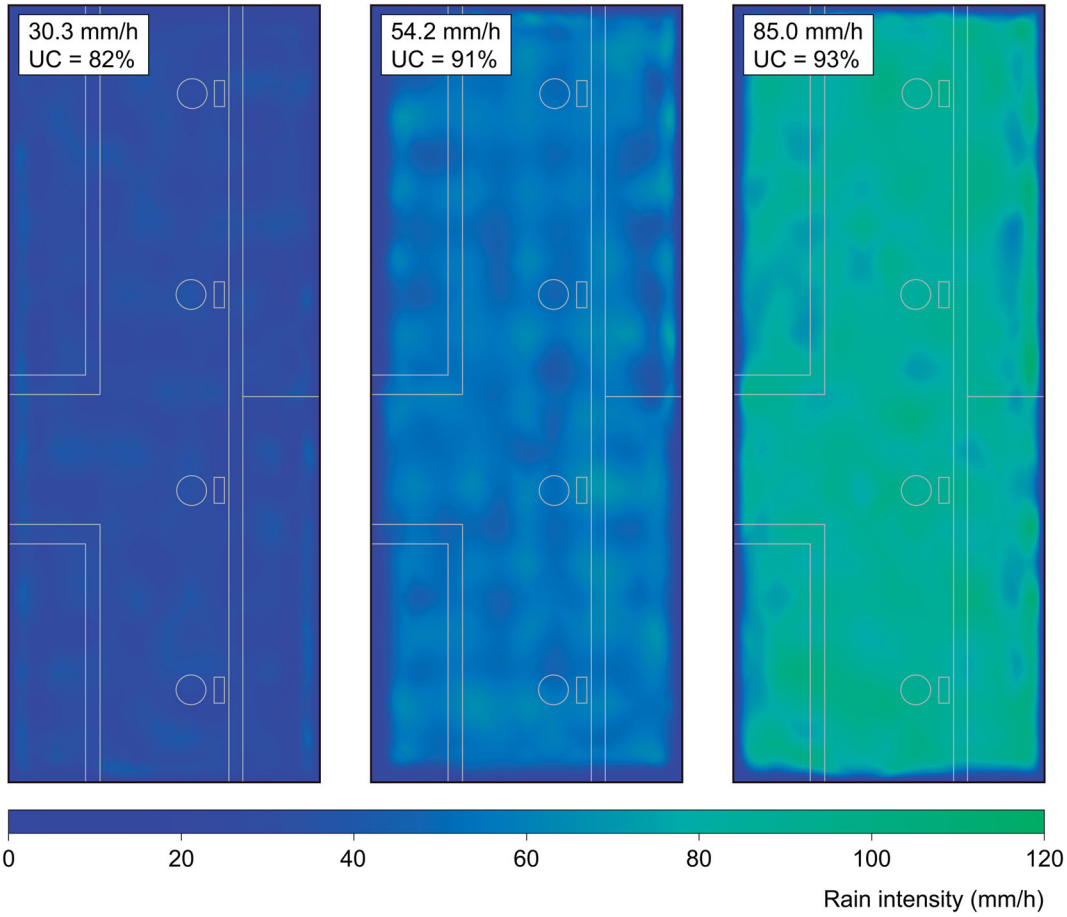


**FIGURE 2** Rainfall intensity maps for the three intensities

surface. The rainfall intensities generated are replicable with a mean absolute error lower than 2 mm/h. In addition, the facility is equipped with instrumentation such as ultrasonic sensors, pressure sensors, and flowmeters. All sensors are connected to a data acquisition system.

In the experimental tests carried out for the present study, only the roofs of the urban drainage facility were used. Four roofs 4.60 m in length ($L$) and 1.55 m wide (but with different slopes) were tested (Figure 1). The projected horizontal width of each roof ($W$) differs slightly from 1.55 m due to the roof slopes. The roofs are made of curved ceramic tiles which are 40.8 cm in length, and with a width of 11.6 cm at their narrow end and 15.0 cm at the wide end. In addition, a smooth roof was reproduced by placing a PVC board over roof 2. All the roofs have a semicircular PVC gutter with a radius of 5.67 cm and a 1% slope. This experimental configuration reflects the dimensions of a wide range of roofs commonly found in practise.

## 2.2 | Characterisation of the rainfall

In order to accurately measure rainfall intensity and its spatial uniformity, a grid of 325 vessels was located over the whole facility. To break the cycles of possible vessel-dripper coincidences, the distance between the vessels was varied between 0.30 and 0.60 m in the transversal direction and between 0.35 and 0.70 in the longitudinal direction. The mass of water captured by the vessels during a period of rain of 10 min was measured to obtain the rain intensity maps shown in Figure 2. The average rain intensities obtained for the three rainfalls that the simulator can generate are 30.3, 54.2, 85.0 mm/h, but in order to simplify the notation, we will refer to these intensities as 30, 50, and 80 mm/h. The spatial uniformity of the rainfall was characterised using Christiansen's uniformity coefficient (Christiansen, 1942):

$$UC = 100\left(1 - \frac{\sum_1^n |\bar{x} - x_i|}{n\bar{x}}\right), \quad (1)$$

where $x_i$ is the rain intensity observed in each vessel, $\bar{x}$ is the average of $x_i$ considering all the vessels, and $n$ is the total number of vessels. The uniformity coefficients obtained for the rainfall intensities of 30, 50, and 80 mm/h were 82%, 91%, and 93%, respectively.

## 2.3 | Topography of the streets and roofs

A detailed 3D surface model of the facility, including the roofs, streets, and pavements was obtained using an Intel® RealSense™

LiDAR Camera L515 sensor. The cloud of data points acquired by the sensor was reconstructed using the scanning software RecFusion 2.1.0, which also allows the user to export the 3D model to standard mesh formats such as polygon file format (PLY). Due to the large size of the experimental facility and the practical limitations on the size of the data that can be managed by the RecFusion software, the facility was split into 10 blocks. The 3D geometry of each block was measured at full-size scale with its own local coordinate reference system. To transform the local coordinates of each block into a global coordinate reference system for the whole facility, a total of 175 reference points, previously obtained through a standard topographic data survey, were used. Once all blocks were globally positioned, they were merged into a unique 3D surface mesh. The transformation from local to global coordinates and the merging of the 10 blocks were carried out using the open source software MeshLab (Cignoni et al., 2008). A rendered representation of the 3D surface mesh reconstruction of the whole facility is shown in Figure 3, although, as previously noted, in this study only the surface runoff on the roofs and gutters was analysed. Finally, a digital elevation model (DEM) to be used in the numerical simulations was obtained from the 3D surface mesh with a 5 mm spatial resolution (Figure 4).

## 2.4 | Experimental laboratory tests

A series of laboratory tests was carried out in the experimental facility in order to measure the hydrographs generated by different rainfall events at the roofs outlets. In addition to the outlet hydrograph for each roof, the water depth was measured at three locations in each gutter.

Six different hyetographs with different intensity and time variability were used in the experiments (Figure 5). The hyetographs H1, H2, and H3 are defined by a constant rainfall intensity of 30, 50, and 80 mm/h, respectively, over the course of 4 min. Hyetographs H4 and H5 represent intermittent rainfall defined by blocks of 15, 30, and 45 s of rain with no-rain intervals of 45 s. Finally, hyetograph H6 consists of a quasitriangular symmetric hyetograph defined by six steps of rainfall of 30 s (Figure 5) and a maximum intensity of 80 mm/h.

In a first stage, a set of experiments was carried out to test the effect of the antecedent moisture condition of the roof tiles. At this stage, roof 2 and roof 3 were tested under constant rainfall intensities for dry and wet antecedent conditions. In the wet antecedent conditions test, the roof tiles were completely wet at the beginning of the experiment. A time lag of 15 min between wet tests was established in order to avoid residual flows from the previous test. On the other

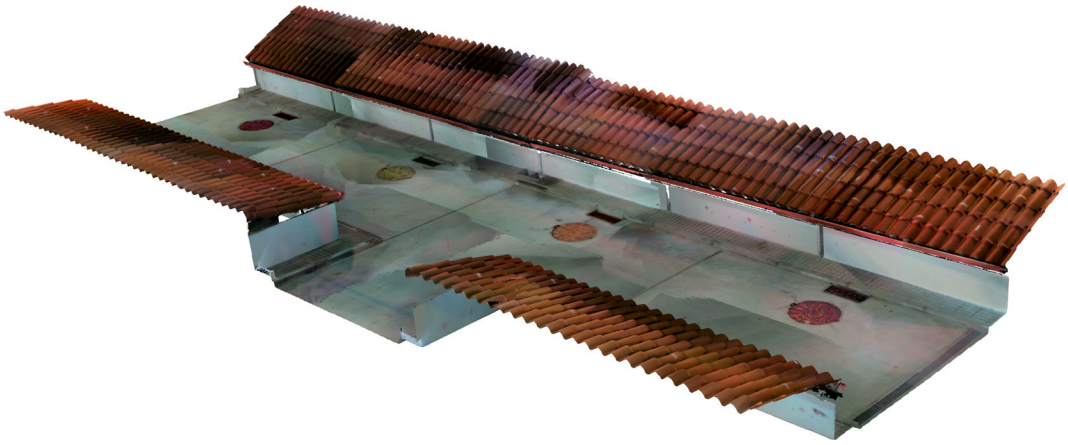

**FIGURE 3** 3D model reconstruction using LiDAR

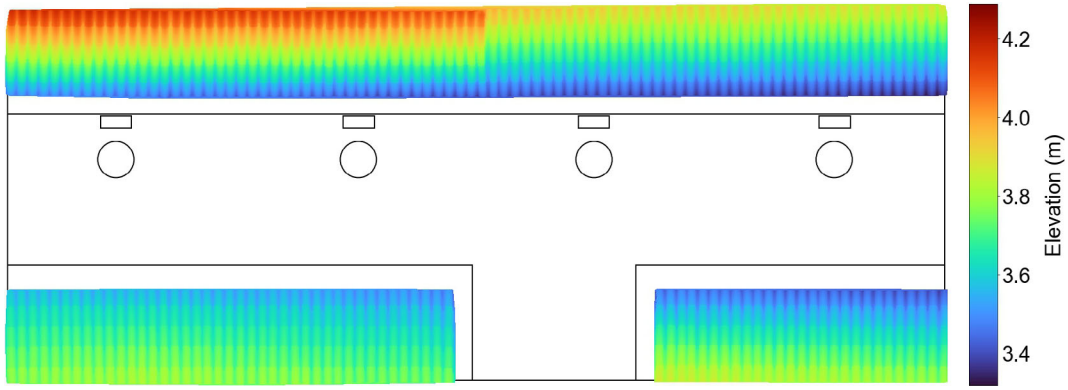


**FIGURE 4** Digital elevation model of the roofs obtained using LiDAR

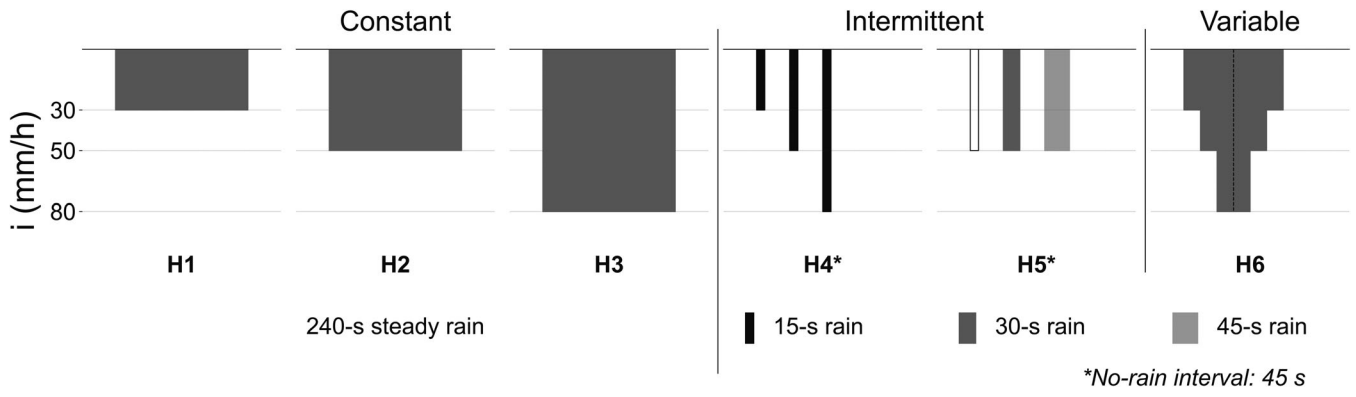


**FIGURE 5** Rainfall hyetrographs used in the experimental tests

**FIGURE 6** Schematic representation of the experimental set up

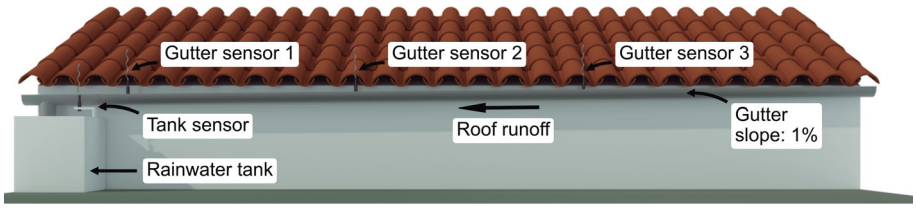


hand, in the dry antecedent condition tests, a dry period of 3 days was left before the beginning of the experiment to guarantees that the tiles were fully dry.

In a second stage, several tests were performed on the four roofs to assess the effect of the roof slope on the outlet hydrograph. Finally, in a last stage, a set of tests using a smooth surface placed over roof 2 (henceforth roof 2P) was carried out to assess the effect of the tiles on the outlet hydrograph. The tests of the second and third stages were carried out for the six hyetographs shown in Figure 5, and for wet antecedent conditions.

The hydrographs at the roofs outlets were measured from the variation of the water level in a square tank with a horizontal cross-section of 0.1225 $m^2$, located at the gutter outlet (Figure 6). The water level in the tank was recorded with a frequency of 5 Hz using an ultrasonic distance sensor (UB500-18GM75-I-V15, Pepperl + Fuchs, Germany) with an output resolution of 0.13 mm. In a similar way, the water depth at 3 locations in the gutters was measured with three ultrasonic sensors, these located at 1.60, 2.85, and 4.10 m from the upstream boundary of the gutter. The experimental setup is shown in Figure 6.

The ultrasonic sensors were previously calibrated to transform the recorded voltage into distance. The raw distance signal was filtered using a low-pass filter in order to remove outliers and to decrease the noise of the signal. Depth increments were computed as the difference between the registered value and the reference depth or zero depth, which was obtained for each test as the mean depth during the first 120 s of the test, before the rainfall starts. Figure 7 shows the processing steps performed in order to obtain the roof outlet hydrograph from the raw signal registered with the ultrasonic sensors.

## 2.5 | Hydraulic modelling

Three approaches with different levels of spatial resolution were used in order to represent the roof in the numerical model: a digital twin approach, a simplified spatial resolution approach, and a lumped approach. In the first two of these approaches the surface runoff over the roofs and gutters was computed with the 2D hydraulic model Iber (Bladé et al., 2014). For the lumped approach, it was implemented in SWMM (Rossman, 2015).

The Iber software solves the 2D depth-averaged shallow water equations using a finite volume solver. The model was initially developed to model river flow, but in recent years several modules have been added to the software that broaden its range of application to hydrological processes (Cea & Bladé, 2015) and urban drainage (Cea et al., 2010; Fraga et al., 2016), amongst others. Iber has been validated in many previous studies (Cea et al., 2014; Cea, Garrido, & Puertas, 2010; Cea et al., 2020). Recently, Iber was linked to SWMM in order to develop a 1D/2D dual drainage model (Sañudo et al., 2020). The 2D depth-averaged shallow water equations solved by the model can be expressed as:

$$\frac{\partial h}{\partial t}+\frac{\partial q_x}{\partial x}+\frac{\partial q_y}{\partial y}=R-i, \tag{2}$$

$$\frac{\partial q_x}{\partial t}+\frac{\partial}{\partial x}\left(\frac{q_x^2}{h}+g\frac{h^2}{2}\right)+\frac{\partial}{\partial y}\left(\frac{q_x q_y}{h}\right)=-gh\frac{\partial z_b}{\partial x}-g\frac{n^2}{h^{7/3}}|q|q_x, \tag{3}$$

$$\frac{\partial q_y}{\partial t}+\frac{\partial}{\partial x}\left(\frac{q_x q_y}{h}\right)+\frac{\partial}{\partial y}\left(\frac{q_y^2}{h}+g\frac{h^2}{2}\right)=-gh\frac{\partial z_b}{\partial y}-g\frac{n^2}{h^{7/3}}|q|q_y, \tag{4}$$

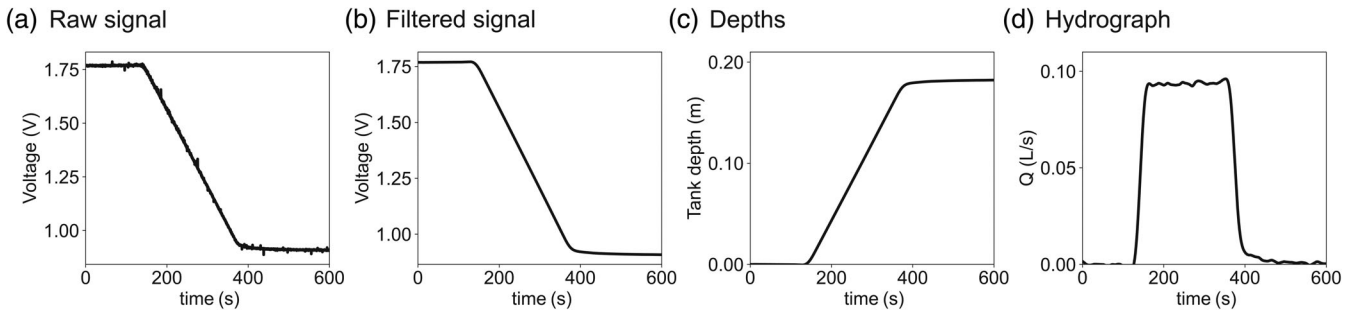


**FIGURE 7** Recorded data processing. (a) Raw signal, (b) filtered signal, (c) depths, and (d) hydrograph

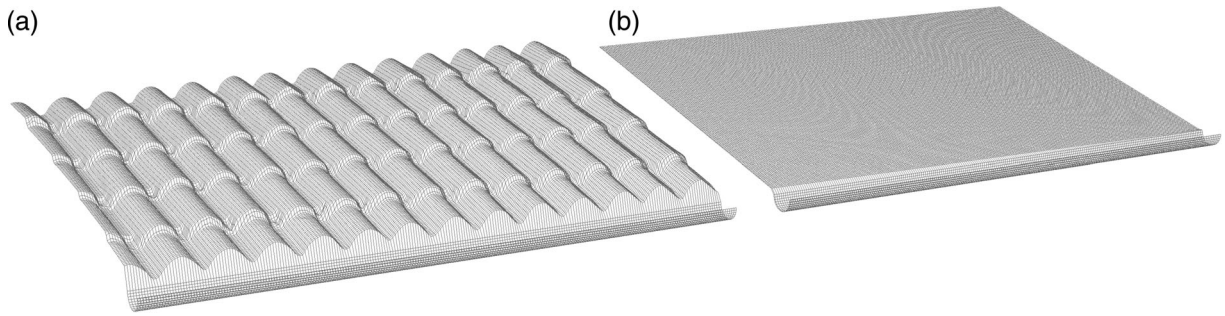


**FIGURE 8** Comparison of the roof domain discretisation used in the 2D analysis. Domain (a) shows the mesh used for the digital twin resolution approach generated through the LIDAR topography. Domain (b) shows the mesh used for the simplified spatial resolution approach generated through a geometry of a sloped plane

where $h$ is the water depth, $q_x$, $q_y$, and $|q|$ are the two components of the unit discharge and its modulus, $z_b$ is the bed elevation, $n$ is the Manning coefficient, $g$ is the gravity acceleration, $R$ is the rainfall intensity, and $i$ is the infiltration rate.

On the other hand, SWMM computes the surface runoff generated by a rainfall event using the nonlinear reservoir method. With this approach, the subcatchment processes are governed by the Manning Equation (5) and the mass continuity Equation (6), the rainfall being considered as the only inflow, and surface runoff, evaporation, and infiltration as the outflows (Rossman & Huber, 2016):

$$Q = \frac{1}{n} \cdot W \cdot S^{1/2} \cdot (d - d_s)^{5/3}, \tag{5}$$

$$\frac{\partial d}{\partial t} = R - e - i - q, \tag{6}$$

where $Q$ is the outlet hydrograph, $n$ is the Manning roughness, $W$ is the subcatchment width, $S$ is the subcatchment slope, $d$ is the depth, $d_s$ is the depression storage depth that fixes the virtual reservoir capacity and sets the initial abstraction, $R$ is the rainfall intensity, $e$ is the evaporation rate, $i$ is the infiltration rate, and $q$ is the runoff rate. In our case study, the evaporation and infiltration were set to zero. It should be noted that outflow only occurs when the depth exceeds the depression storage and the slope is different from zero.

For the digital twin and simplified spatial resolution approaches, each roof was discretized using a structured mesh with an average element size of 0.01 m and around 73 000 elements. All the simulations were performed using a wet-dry threshold of 0.01 mm and the DHD scheme (Cea & Bladé, 2015). Figure 8 compares the computational meshes used in the digital twin and simplified spatial resolution approaches. The digital twin topography was obtained from the DEM shown in Figure 4, whereas the simplified spatial resolution topography is a plane with a slope equivalent to that of the digital twin. In the lumped approach each roof was considered as a single subcatchment with no evaporation and no infiltration, a width equal to 4.6 m, and with the average slope of the roof.

## 3 | RESULTS AND DISCUSSION

### 3.1 | Roof initial abstraction

The initial abstraction is defined as the rainfall needed to wet the roof surface and fill its small irregularities before the beginning of the surface runoff. The initial abstraction in the experiments was estimated as the difference between the volume of the hydrographs measured under wet and dry initial conditions (Figure 9). The values obtained vary between 0.2 and 0.4 mm. These values are slightly smaller than the value of 0.8 mm obtained by Farreny et al. (2011) for a sloped clay tile roof located in an outdoor environment. Such a difference may be justified by the difference between laboratory and field conditions regarding climatology (e.g., wind effect), uncertainty on rain measures, or the state of

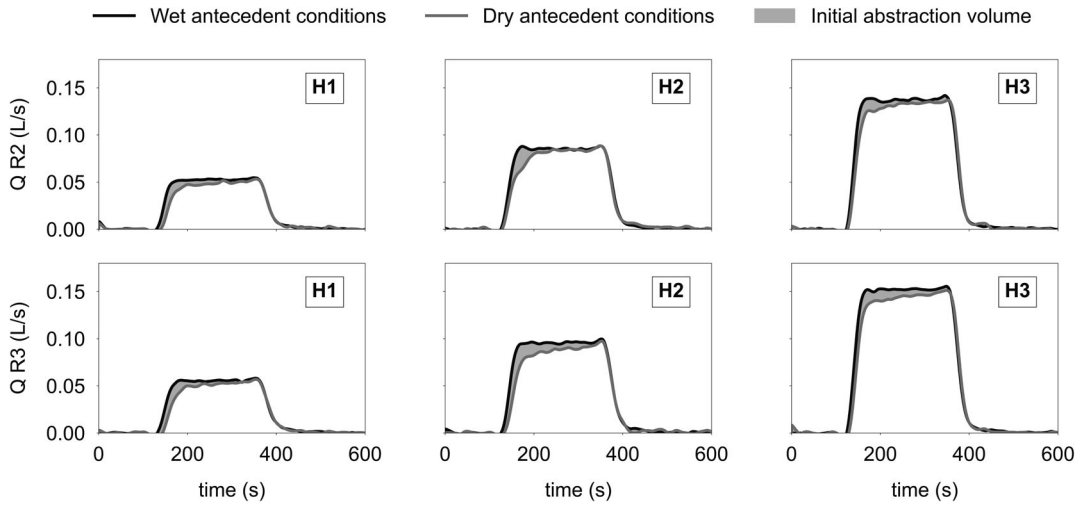


**FIGURE 9** Hydrographs measured for wet and dry antecedent conditions in roofs R2 (up) and R3 (down) for the three constant rainfalls of 30 (H1), 50 (H2), and 80 (H3) mm/h

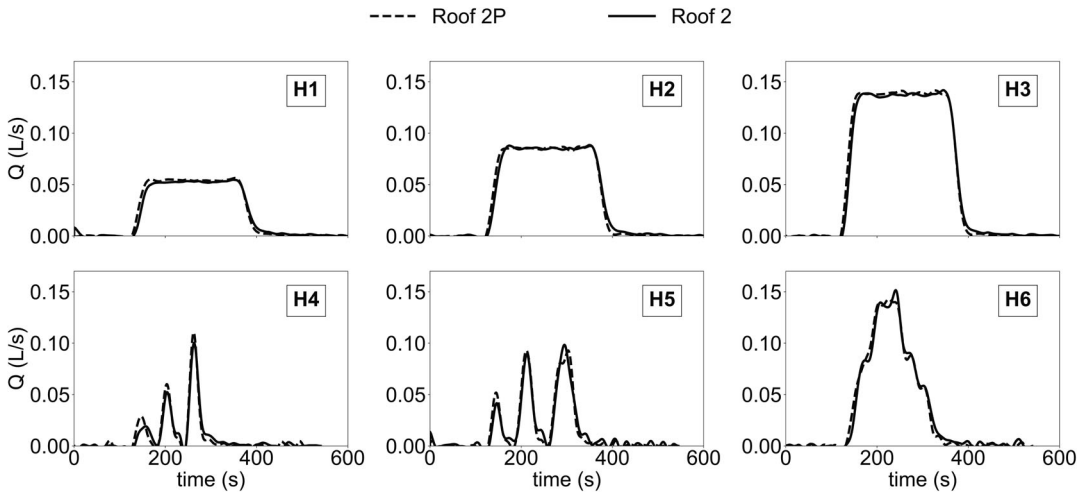


**FIGURE 10** Experimental hydrographs for plain (roof 2P) and tile (roof 2) roof surfaces

conservation of the roof. In any case, these values suggest that for practical purposes the initial abstraction can be excluded from consideration.

## 3.2 | Experimental hydrographs for tile and plain roofs

The effect of the shape of the tiles on the outlet hydrograph is shown in Figure 10, which compares the outlet hydrographs observed in roof 2 with its original configuration (tiles) and in Roof 2P (smooth plain surface over the roof). The mean absolute difference (MAD) between both hydrographs is lower than 0.005 L/s for all tests, which is roughly a 5% of the peak discharge. Thus, the experimental results do not show significant differences between the two types of roof surface, and hence the shape of the tiles does not play a significant role in the rainfall-runoff transformation.

## 3.3 | Effect of the roof slope on the outlet hydrograph

The outlet hydrographs measured on the 4 roofs for the 6 hyetographs are shown in Figure 11a. It should be noted that, although the four roofs had the same dimensions, not all roofs received exactly the same volume of rain due to the small difference between the horizontal projected areas and the slight spatial variability of the rainfall intensity over each roof. Thus, to better visualise the difference between the rising and falling limbs, the observed hydrographs were normalised by the steady discharge, obtained as the value of the peak intensity of the hyetograph multiplied by the roof area. The dimensionless hydrographs are shown in Figure 11b. No significant differences were observed between the hydrographs, except some small differences in the rising and falling limbs, where a lower roof slope produced a slightly smoother limb.

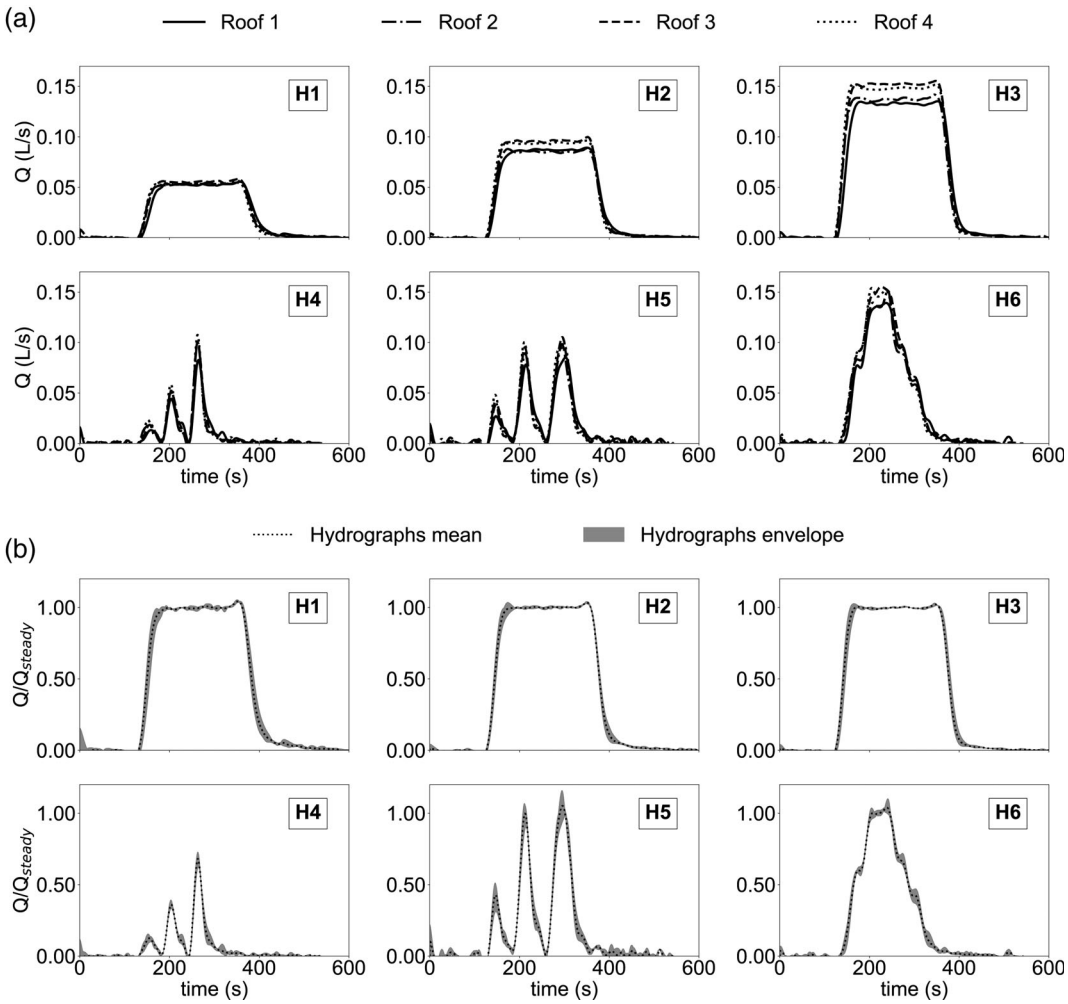


**FIGURE 11** Roof hydrographs (a) and roof dimensionless hydrographs (b) for the six hyetographs

**TABLE 1** Summary of the three levels of detail analysis and of the numerical models

| Level of detail | Software | Geometry | Manning | |
|---|---|---|---|---|
| | | | Roof | Gutter |
| Digital twin | Iber | 2D mesh | 0.025 | 0.015 |
| Simplified spatial resolution | Iber | 2D mesh | 0.025 | 0.015 |
| Lumped approach | SWMM | Subcatchment | 0.025 | - |

## 3.4 | Calibration and comparison of the three modelling approaches

The three numerical approaches used in this study use the Manning coefficient to represent the roughness of the roof surface. Therefore, the Manning coefficient was manually calibrated for the three approaches, by fitting the rising and falling limbs of the numerical and experimental hydrographs. The calibration was carried out for the four roofs using hyetographs H4 and H5. Since the calibration was done for the experiments with wet antecedent conditions, the initial abstraction and depression storage depth ($d_s$ in Equation (5)) was set to zero. The Manning of the roof and gutter were calibrated jointly in order to maximise the Nash-Sutcliffe efficiency coefficient (NSE). The Manning was varied using a range between 0.015 and 0.050. For the digital twin approach, the best fit to the experimental hydrographs was obtained with a Manning coefficient of 0.025. The calibrated Manning for the simplified spatial resolution and lumped approach was also 0.025. The Manning coefficient obtained for the gutter was 0.015. Table 1 shows a summary of the main features for the three approaches.

Figure 12 shows the results obtained with the digital twin approach compared to the experimental observations. In addition to the NSE, the value of the mean absolute error (MAE) is provided.

The high resolution of the numerical modelling with the digital twin topography makes it possible to see the flow path throughout the tile channels, as shown in Figure 13.

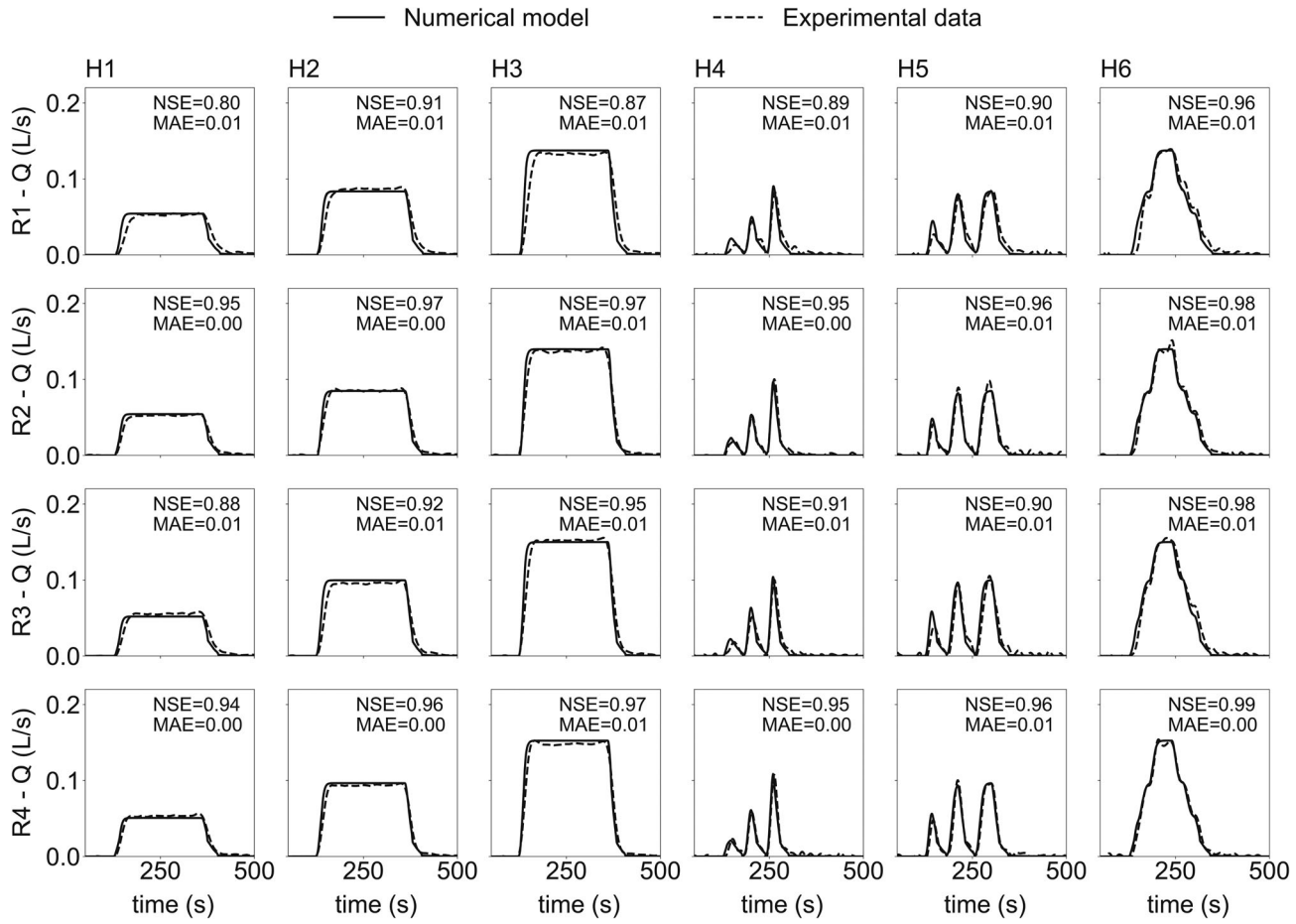


**FIGURE 12** Comparison of the numerical and experimental results obtained with the digital twin approach for the six hyetographs

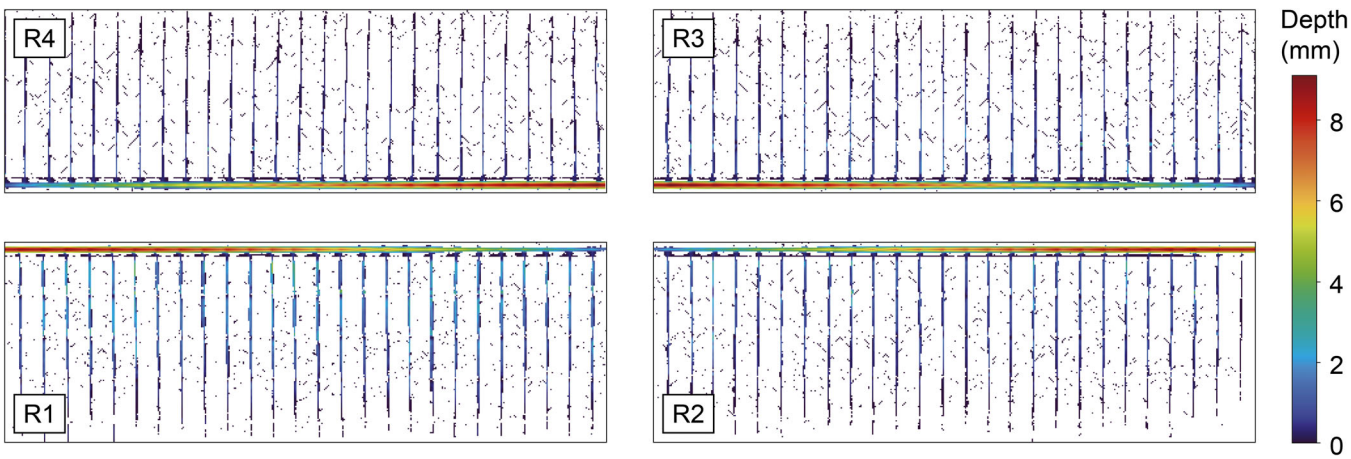


**FIGURE 13** Depth map on roofs for the digital twin resolution

The comparison of the depths measured and computed in the gutter of roof 2 for the depth sensor 2 (Figure 6), located at 2.85 from the upstream boundary of the gutter, is shown in Figure 14. These results validate the good performance of the model in computing the physics of roof processes even for very low depths. The average MAE for the 24 experiments is 0.8 mm. It can be noted that once the rainfall finishes, the depths did not become zero, since the gauge measures the water that remains in the gutter due to surface tension.

In order to assess whether the extra modelling and computational efforts required by the digital twin approach are worthwhile, the

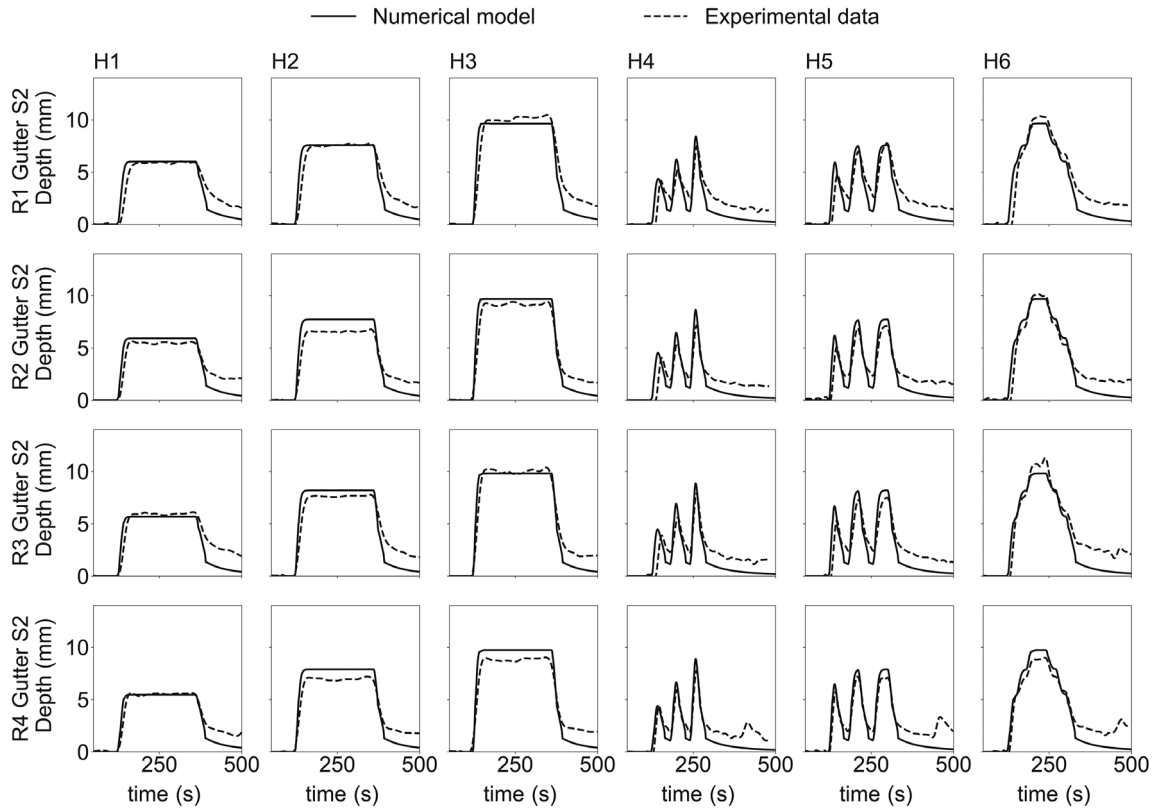


**FIGURE 14** Numerical and experimental comparison of water depths at gutter sensor 2 of roof 2 modelled with the digital twin approach

simplified resolution and lumped approaches were computed with a roof and gutter using a Manning coefficient of 0.025 and 0.015, respectively. The comparison between the hydrographs of the digital twin and the simplified spatial resolution gives an average NSE = 0.97 and an average MAE = 0.002 L/s. On the other hand, Figure 15 shows that there are no significant differences between the digital twin model and the lumped approach. For intermittent rainfalls (H4 and H5), the first peak of the lumped approach differs from the 2D analysis specially for low roof slopes. This is caused by the poor performance of the nonlinear reservoir method for rainfalls with duration less than the time of concentration of the roof (Xiong & Melching, 2005). Thus, the lumped approach performs better when the time of concentration of the roofs is less than the rainfall duration, which is the case in most real applications, in which the rainfall duration usually exceeds the time of concentration of a typical roof, so the use of the nonlinear reservoir method is justified. The comparison, then, illustrates the good performance of the sloped planed simplification and of the nonlinear reservoir method for modelling roof hydraulic processes.

The nonlinear reservoir or lumped approach has significant advantages in terms of a full 2D hydraulic analysis, especially the decreased computational time required due to the simplicity of the approach. This is an important finding, since 1D-2D urban drainage models need fine meshes to achieve reliable results, which have a high impact on computational time.

## 3.5 | Modelling of full-size roofs

### 3.5.1 | Effect of modelling approaches and roof slope

The roofs of the experimental facility analysed in the previous sections represent real roofs in terms of design and materials but with smaller dimensions, implying shorter concentration times. Therefore, a set of numerical experiments was carried out on roofs with larger dimensions in order to characterise their hydrologic behaviour and to evaluate the differences between the lumped and the 2D distributed approaches. A total number of 45 roofs of different sizes and slopes were modelled, resulting from the combination of 3 widths (1.55, 5, and 8 m), 3 lengths (4.6, 10, and 15 m) and 5 slopes (2%, 16%, 26%, 37%, and 51%). The width and length dimensions cover the range typically found in urban roofs. The five slopes are those of the experimental facility plus an additional 2% slope that represents a typical flat roof. The numerical analysis was done with both, the 2D distributed approach that considers the roof as a sloped plane and includes the gutter explicitly, and the lumped approach. Both approaches follow the methodology described in Section 2.5, but to reduce the computational effort the resolution of the computational mesh was reduced to 0.05 m, after verifying that the effect on the results was negligible. Figure 16 compares the concentration time for the 2D and lumped approaches for the different dimensions and slopes analysed.

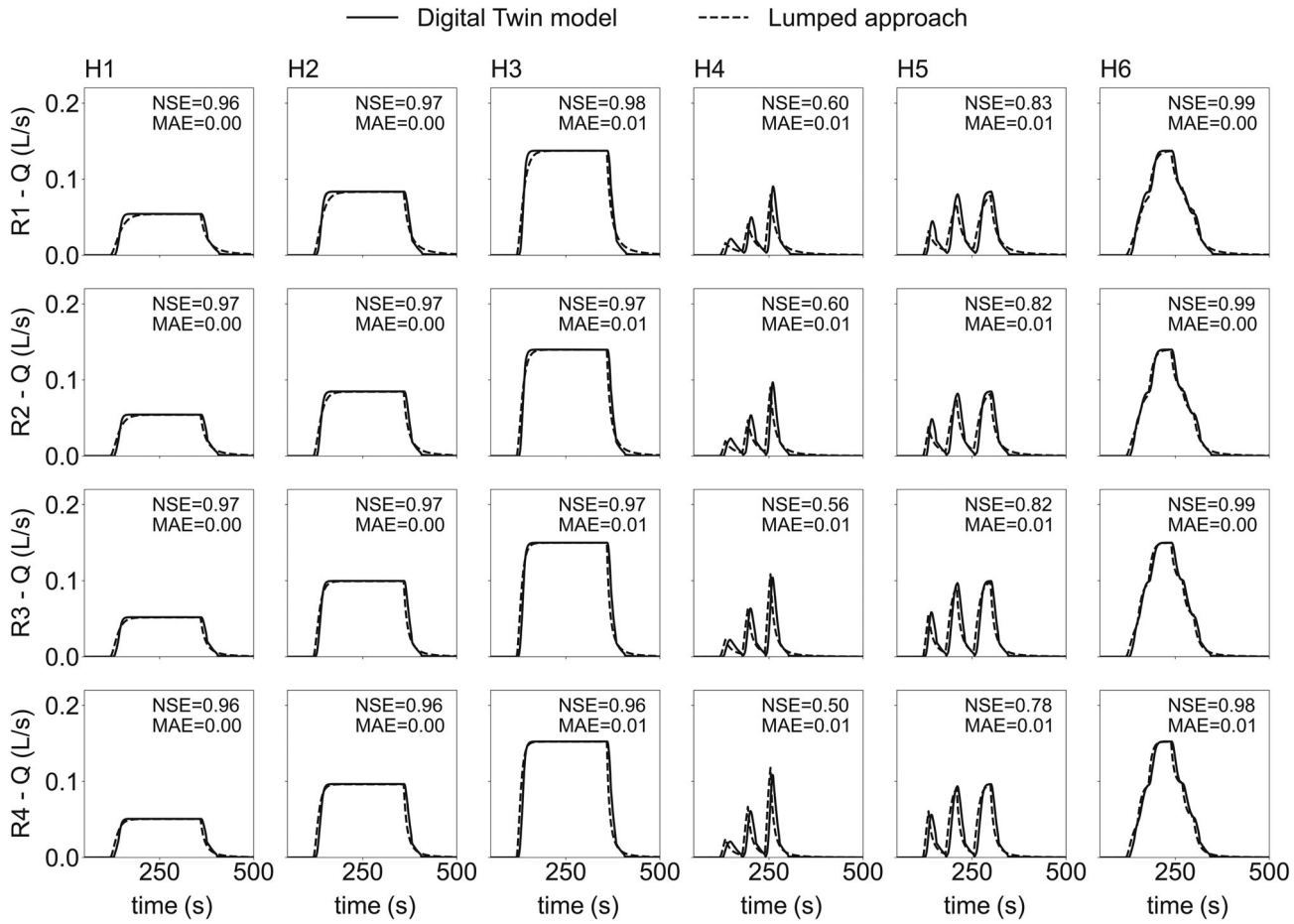


**FIGURE 15** Comparison of the numerical hydrographs for the digital twin model and the lumped approach

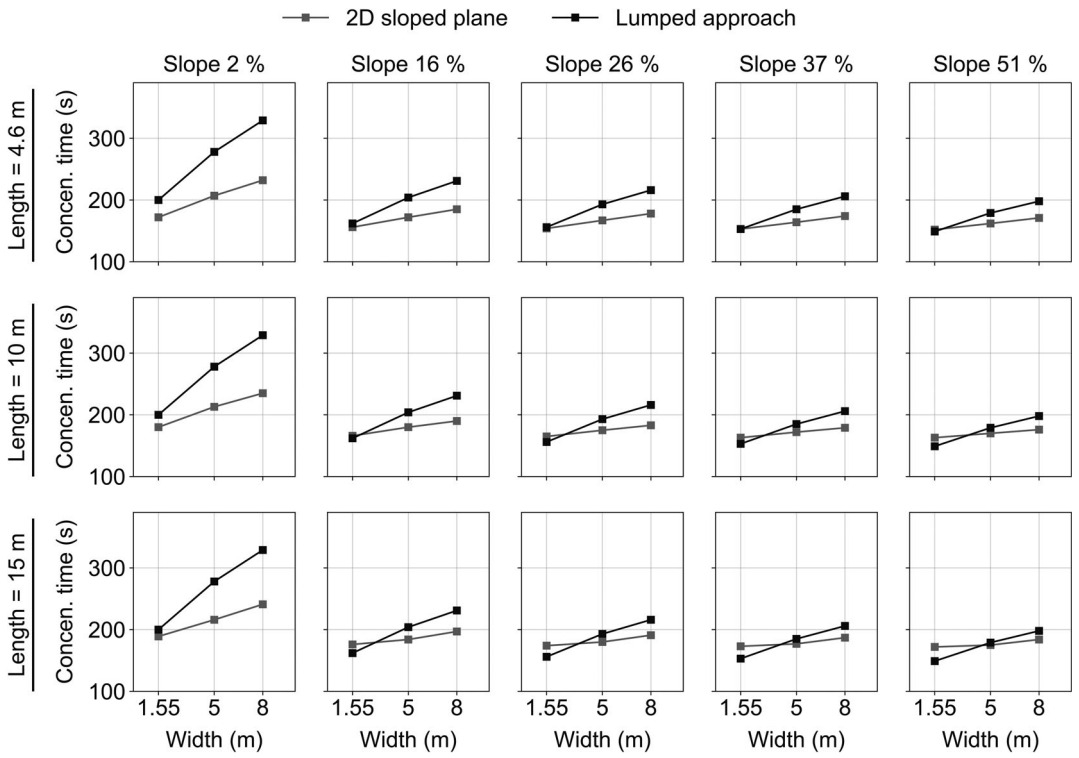


**FIGURE 16** Concentration time for the 2D sloped plane approach and the lumped approach for different roof lengths, widths, and slopes

The numerical results show that the largest differences occur for the slope of 2%, where the difference in the concentration time computed with both approaches reaches 96 s in the largest roof. For practical purposes in an urban drainage model of a whole urban district this difference is small compared to the time resolution of the rainfall data, which is usually between 5 and 10 min. For the rest of slopes the differences are of the order of seconds, even for the largest roof, and they decrease as the slope increases.

The effect of the slope on larger roofs is summarised in Figure 17. Results show that the differences on the concentration time for the roofs with slopes from 16% to 51% are negligible when modelling with the 2D sloped plane approach, and of the order of seconds when

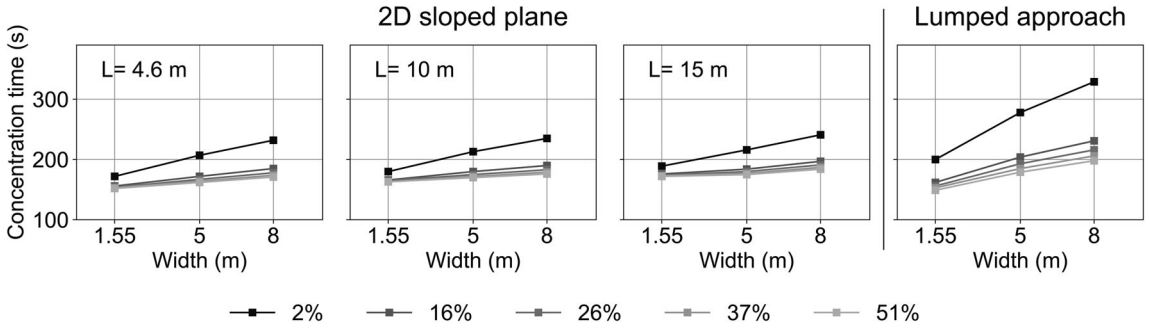


**FIGURE 17** Concentration time for 2D sloped plane approach and the lumped approach sorted by roof slopes

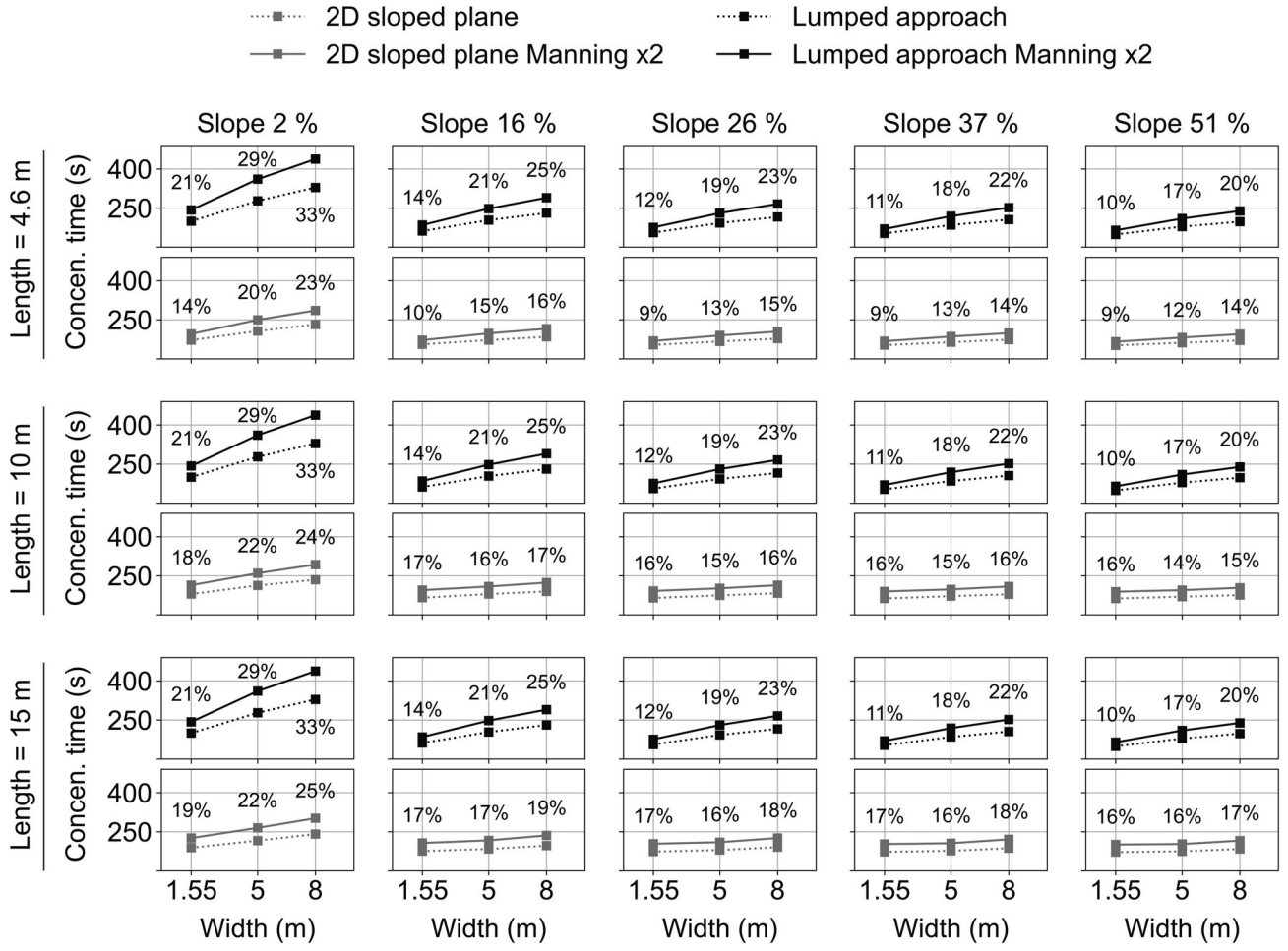


**FIGURE 18** Concentration time for each roof configuration sorted by length, width, and slope for the 2D sloped plane approach and for the lumped approach. The dotted lines represent the base analysis and the solid line the results by multiplying the manning coefficient by 2. The percentage label expresses the concentration time increment due to an increased surface roughness

modelling with the lumped approach. Note that with the lumped approach the concentration time does not depend on the length of the roof, but only on its width (Equation (5)). The slope of 2% presents a slightly different behaviour. In that case, the highest differences are upper than 100 s with regard to the other slopes for the largest roof modelled with the lumped approach. This suggests that for practical purposes, the roofs can be grouped into flat roofs and sloped roofs.

### 3.5.2 | Sensitivity to surface roughness

The surface roughness coefficient used to model the surface runoff in the roofs analysed in the previous sections is representative of new and clean surfaces. These conditions are not the usual ones in real roofs that are exposed to atmospheric conditions. Material ageing under outdoor conditions will produce an increase in surface roughness due to the presence of grass and earth on the roofs and gutters. In order to assess this effect, the tests shown in Figure 16 were replicated increasing the roof and gutter Manning coefficients from 0.025 to 0.050, and from 0.015 to 0.030, respectively. Figure 18 shows the increase on the concentration time caused by an increase in the surface roughness. The sensitivity to the Manning is higher in the lumped approach and for small roof slopes, with a maximum increment of 33%. In the case of the 2D sloped plane, the differences are in general smaller than 20%. Despite multiplying by a factor 2 the Manning coefficient, which implies a very high surface roughness, the increment on the concentration time does not seem very relevant for models at the urban catchment scale.

## 4 | CONCLUSIONS

A series of experiments were carried out under laboratory-controlled conditions to characterise the rainfall-runoff transformation over roofs. The experimental tests were replicated numerically using three different approaches with different resolutions: a digital twin approach with a high-resolution topography, simplified spatial resolution geometry, and a lumped approach. In addition, a numerical analysis was carried out on larger roofs to assess the effect of the roof size on the outlet hydrograph. From the results the following conclusions can be drawn:

- The initial abstraction of the roofs estimated from the experimental tests varied between 0.2 and 0.4 mm.
- The experimental and numerical hydrographs show no significant sensitivity to the roof slope except for the case of flat roofs (2% slope) which presents significantly larger concentration times than sloped roofs. The same occurs with the tiles, in that a faithful representation of the roof does not change the results considerably.
- A Manning coefficient of 0.025 presents the best fit for the three modelling approaches. Sensitivity to the Manning coefficient does not seem significant for roof modelling at the urban catchment scale.
- Although 2D models represent the rainfall-runoff processes better, for practical purposes their complexity in terms of input data, discretisation, and computational time does not justify their application. The lumped approach computed with the nonlinear reservoir method is therefore more appropriate for modelling roofs in urban drainage models.

## ACKNOWLEDGEMENTS

This work was supported by the Spanish Ministry of Science and Innovation (Ministerio de Ciencia e Innovacion) within the project "SATURNO: Early warning against pluvial flooding in urban areas" [grant number PID2020-118368RB-I00]. Funding for open access charge: Universidade da Coruña/CISUG.

## DATA AVAILABILITY STATEMENT

Data sharing is not applicable to this article as no new data were created or analyzed in this study.

## ORCID

*Esteban Sañudo* https://orcid.org/0000-0003-3200-114X
*Luis Cea* https://orcid.org/0000-0002-3920-0478
*Jerónimo Puertas* https://orcid.org/0000-0001-6502-0799

## REFERENCES

Bladé, E., Cea, L., Corestein, G., Escolano, E., Puertas, J., Vázquez-Cendón, E., Dolz, J., & Coll, A. (2014). Iber: Herramienta de Simulación Numérica Del Flujo En Ríos. *Revista Internacional de Metodos Numericos Para Calculo y Diseno En Ingenieria*, *30*(1), 1–10.

Cao, X., Qi, Y., & Ni, G. (2021). Significant impacts of rainfall redistribution through the roof of buildings on urban hydrology. *Journal of Hydrometeorology*, *22*(4), 1007–1023.

Cea Gómez, L., Bladé i Castellet, E., Sanz Ramos, M., Fraga, I., Sañudo Costoya, E., García-Leal, O., Gómez-Gesteira, M., & González-Cao, J. (2020). Benchmarking of the Iber capabilities for 2D free surface flow modelling.

Cea, L., & Bladé, E. (2015). A simple and efficient unstructured finite volume scheme for solving the shallow water equations in overland flow applications. *Journal of the American Water Resources Association*, *5*(3), 2–5486.

Cea, L., Garrido, M., & Puertas, J. (2010). Experimental validation of two-dimensional depth-averaged models for forecasting rainfall-runoff from precipitation data in urban areas. *Journal of Hydrology*, *382*(1–4), 88–102.

Cea, L., Garrido, M., Puertas, J., Jácome, A., Del Río, H., & Suárez, J. (2010). Overland flow computations in urban and industrial catchments from direct precipitation data using a two-dimensional shallow water model. *Water Science and Technology*, *62*(9), 1998–2008.

Cea, L., Legout, C., Darboux, F., Esteves, M., & Nord, G. (2014). Experimental validation of a 2D overland flow model using high resolution water depth and velocity data. *Journal of Hydrology*, *513*, 142–153.

Chang, T. J., Wang, C. H., & Chen, A. S. (2015). A novel approach to model dynamic flow interactions between storm sewer system and overland surface for different land covers in urban areas. *Journal of Hydrology*, *524*, 662–679.

Christiansen, J. E. (1942). *Irrigation by sprinkling*. Agricultural Experiment Station, University of California.

Cignoni, P., Callieri, M., Corsini, M., Dellepiane, M., Ganovelli, F., & Ranzuglia, G. (2008). MeshLab: An open-source mesh processing tool. Proceedings of the 6th Eurographics Italian Chapter Conference (pp. 129–136).

Farreny, R., Morales-Pinzón, T., Guisasola, A., Tayà, C., Rieradevall, J., & Gabarrell, X. (2011). Roof selection for rainwater harvesting: Quantity and quality assessments in Spain. *Water Research*, *45*(10), 3245–3254.

Fraga, I., Cea, L., & Puertas, J. (2017). Validation of a 1D-2D dual drainage model under unsteady part-full and surcharged sewer conditions. *Urban Water Journal*, *14*(1), 74–84.

Fraga, I., Cea, L., Puertas, J., Suarez, J., Jimenez, V., & Jacome, A. (2016). Global sensitivity and GLUE-based uncertainty analysis of a 2D-1D dual urban drainage model. *Journal of Hydrologic Engineering*, *21*(5), 04016004.

Leandro, J., & Martins, R. (2016). A methodology for linking 2D overland flow models with the sewer network model SWMM 5.1 based on dynamic link libraries. *Water Science and Technology*, *73*(12), 3017–3026.

Naves, J., Anta, J., Suárez, J., & Puertas, J. (2020). Development and calibration of a new dripper-based rainfall simulator for large-scale sediment wash-off studies. *Water (Switzerland)*, *12*(1), 152.

Pina, R. D., Ochoa-Rodriguez, S., Simões, N. E., Mijic, A., Marques, A. S., & Maksimović, Č. (2016). Semi- vs. fully-distributed urban stormwater models: Model set up and comparison with two real case studies. *Water (Switzerland)*, *8*(2), 58.

Rossman, L. A. (2015 September). Storm water management model user's manual version 5.1'. EPA/600/R-14/413b (p. 352). National Risk Management Laboratory Office of Research and Development. United States Environmental Protection Agency, Cincinnati, Ohio.

Rossman, L. A., & Huber, W. C. (2016 January). Storm water Management model reference Manual volume I – Hydrology (revised)(EPA/600/R-15/162A) (p. 231). U.S. Environmental Protection Agency I.

Sañudo, E., Cea, L., & Puertas, J. (2020). Modelling pluvial flooding in urban areas coupling the models iber and SWMM. *Water (Switzerland)*, *12*(9), 2647.

Silveira, A., Abrantes, J. R. C. B., De Lima, J. L. M. P., & Lira, L. C. (2016). Modelling runoff on ceramic tile roofs using the kinematic wave equations. *Water Science and Technology*, *73*(11), 2824–2831.

Xiong, Y., & Melching, C. S. (2005). Comparison of kinematic-wave and nonlinear reservoir routing of urban watershed runoff. *Journal of Hydrologic Engineering*, *10*(1), 39–49.

**How to cite this article:** Sañudo, E., Cea, L., & Puertas, J. (2022). Comparison of three different numerical implementations to model rainfall-runoff transformation on roofs. *Hydrological Processes*, *36*(5), e14588. https://doi.org/10.1002/hyp.14588